ULB BRUFACE BRUSSELS FACULTY OF ENGINEERING VUB

ELEC-H415 - Communication channels

Project

Channel modeling for 5G small cells

Authors:

John Antoun

Dejvi Cakoni

Olivier Ducastel

Pietro Marzio

Professor:

Philippe De Doncker

Teacher assistant:

Guylian Molineaux

June 15, 2020

Contents

1 Introduction

The advent of 5G systems has introduced a new frequency spectrum of high bandwidth that goes under the millimeter wave spectrum. Adopting these bands brings two main benefits. First, most of these bands are unutilized and they are free, thus there are no interferences with other technologies. Second, a large bandwidth offers higher data rates for all users, as there are higher numbers of users who are connected in a small geographical area, which is also stated as the Internet of Things (IoT). However, high-frequencies bands open several challenges in terms of signal attenuation, coverage area limitations, path and penetration losses, scattering and so on. In addition of this, these waves are susceptible to blockage from buildings and other structures, particularly in higher-density urban areas. To optimize the communication efficiency between a transmitter (Tx) and a receiver (Rx), an identification of the channel performance at a given frequency is required. Therefore, this report investigates the potential ability of some path lose models for given assumptions.

2 Scenario

In order to model the downlink channel, some assumptions have been taken to meet the results required. To implement the whole scenario, a C++ code was written through the software *Qt*. A small street delimited by buildings and with crossing streets was designed. The street is discretized in a grid of $1m^2$ zones for which all parameters are computed. The Tx and the Rx are modelled as half-wave dipoles antenna. They were positioned at the same height above the ground and, based on the situations, they were moved on around the street to study different cases: Line-of-Sight (LOS) or Not-Line-of-Sight (NLOS), with up to three reflections on building walls. The table

below shows the parameters taken into account:

	Scenario
Carrier frequency	$26GHz$
Bandwidth	$\leq 200MHz$
Relative permittivity	$3 \leq \epsilon \leq 5$
$EIRP_{MAX}$	$2W$
Target SNR at receiver	$8dB$
Receiver noise figure	$10dB$
Interference margin	$6dB$
Minimal distance to the base station	$10m$

Additionally, only the path loss and fading will be considered due to the simple scenario, discarding the shadowing effect.

3 Image method and diffraction algorithm

The image method aims to find all reflection paths possibilities between a Tx and a Rx by an iterative process. Considering a wall, when a ray is reflected, an image Tx spawns as the original Tx is mirrored in the surface. This mirror of Tx is useful because the distance between it and the Rx is the total distance from the original Tx to Rx while reflecting on the wall. Further reflections are found by mirroring again the mirror image of Tx until all possible combinations are found. A representation of it can be found on the lecture notes, Fig. 3.10 and 3.11.

$$P_{RX} = \frac{1}{8R_a} \left| \sum_{n=1}^{N} \underline{h_e}(\theta) \cdot \underline{E_n} \right|^2 \tag{1}$$

The algorithm implemented can be found as *imageMethod5G*, a function in the *mainwindow.cpp* and is based on the image method, as well on equation

(1)[1]. This function takes some arguments as inputs that actually are the representation of the spatial environment needed. Hereafter, a variable *sum* is initialised to make the sum of equation 1. This variable is the core of all the computations: it is updated every time the algorithm finds a set of possible reflections (and compute the coefficients and complex exponential of equation 3.52 of the lecture notes).

The algorithm is divided in two main steps. The first one checks if the Tx and the Rx are in LOS. If yes, the direct wave is computed to update *sum* according to the distance. Otherwise (NLOS), diffraction is computed in the second branch of the first step using the equations of a generalisation of the *knife-edge* model[2]. As can be seen in Fig.1, virtual walls have been added (in grey inside the buildings) to establish a diffraction scheme between two NLOS antennas. The algorithm checks both extremities of each virtual wall, and if the line between the extremity and the receiver (or transmitter) meets an obstacle, this extremity is discarded for diffraction. If diffraction is allowed to happen, all parameters for diffraction (s1,s2,Δr, etc) can be found with the virtual wall[3].

The second step concerns the computations of the other rays reflected on the buildings, up to three times. This is done by checking if the Tx and the Rx are on the same side of the wall considered. Once this is verified, the first reflection term is computed evaluating the LOS conditions for the reflected point on the wall. The same idea is applied for the second and the third reflection, discarding the wall previously considered.

All along the algorithm the delays and attenuations are stored into vectors, useful to evaluate the impulse responses or spectrum. In the end, this

[1]Eq. 3.51 of the lecture notes

[2]Course notes section 3.3.3.

[3]The fact that both extremities are checked for diffraction is also useful if the wall is placed in the middle of the street to mimic an obstacle on which diffraction happens from both extremities.

function returns the variable *sum* into the *MainWindow* function to compute the power received P_{RX} (1).

Then, the results are elaborated to have a graphical visualisation and print of various communication data (SNR,power, delay spread, etc).

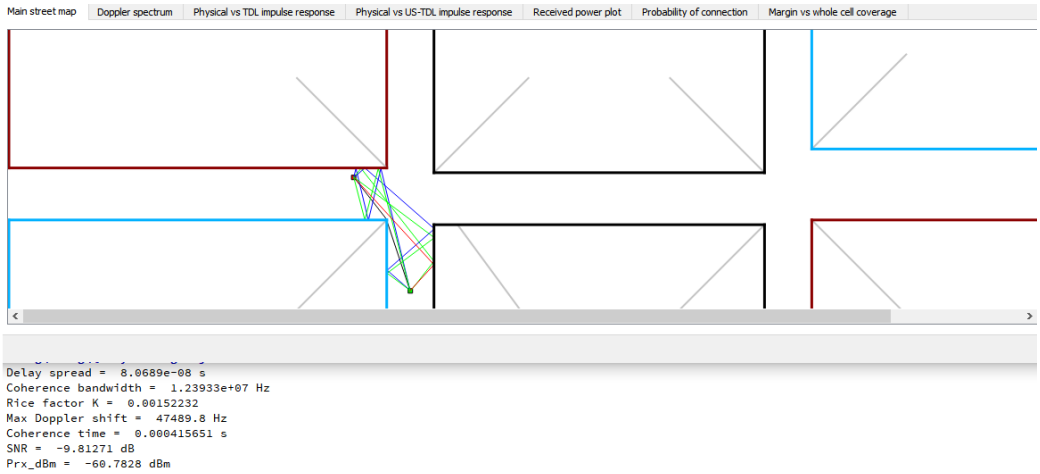

Figure 1: Simulation example

3.1 Validation on basic examples

Here below are shown two basic examples computed by hand to validate the results obtained through the C++ code.

3.1.1 Reflections

The *urban canyon* model has been considered to compute the reflections. Some arbitrary assumptions have been taken: the Tx and the Rx are at the same height $h = 1.6m$ above the ground and also in the middle of the street with width $2w = 10m$ delineated by the buildings with their relative permittivity $\epsilon = 5$ (the same as the ground). The distance between the Tx and the Rx is $d = 30m$. Six rays have been considered: the direct wave, the

ground reflected wave and two buildings reflected waves for each side of the street. Equations 3.23, 3.24, 3.25, 3.54 of the lecture notes have been used to compute the geometry and the coefficients behind the model. The numerical results are shown in the table below:

	Reflections coefficients	Total distances	Angles
Ground ray	$\Gamma_{\parallel} = -0,58$	$d_g = 30,17m$	$\theta_g = 83,91°$
1 time reflected ray	$\Gamma_{\perp 1} = -0,85$	$d_1 = 30,41m$	$\theta_1 = 80,53°$
2 times reflected ray	$\Gamma_{\perp 2} = -0,73$	$d_2 = 31,62m$	$\theta_2 = 71,56°$

Thus the total P_{RX} (1) becomes:

$$P_{RX,LOS} = \frac{1}{8R_a}\left(\frac{\lambda}{\pi}\right)^2 (60 \cdot EIRP)\Big|\frac{e^{-j\beta d}}{d} + \frac{cos\left(\frac{\pi}{2}cos(\theta_i)\right)}{sin^2(\theta_i)}\frac{\Gamma_{\parallel}(\theta_g)}{d_g}e^{-j\beta d_g} + \\ +2\Gamma_{\perp 1}\frac{e^{-j\beta d_1}}{d_1} + 2\Gamma_{\perp 2}^2\frac{e^{-j\beta d_2}}{d_2}\Big|^2 \tag{2}$$

where:

- $R_a = 73\Omega$ (the radiation resistance of the dipole)
- $\lambda = c/f$ (wavelength)
- $\beta = (2\pi f)/c$
- $\theta_i = \theta_g - \pi = 83,91°$

Substituting all the coefficients and parameters, the total power received in dBm is:

$$P_{RX,LOS,dBm} = 10\log_{10}\left(\frac{P_{RX,LOS}}{0.001}\right) \simeq -52,7833[dBm] \tag{3}$$

Then, the same parameters were adopted into the C++ code that gives the results depicted in Fig. 2 shown below:

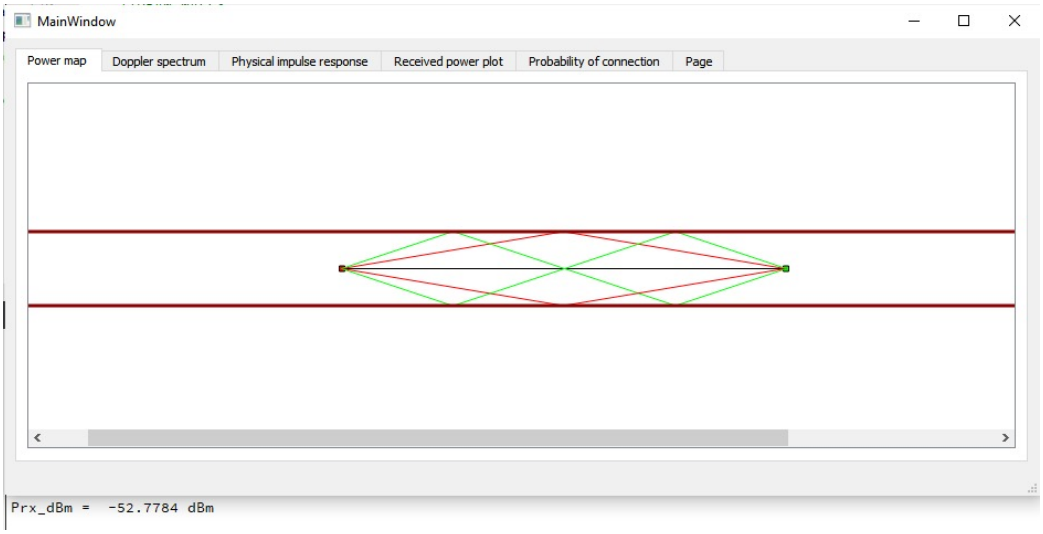

Figure 2: Reflections results on Qt

As one can see, the results match the computed value.

3.1.2 Diffraction

For the diffraction case, the *knife-edge* model has been considered. Again, as before, some arbitrary assumptions have been taken: the Tx and the Rx at the same height $h = 1.6m$ above the ground but this time they are positioned in such a way to have the NLOS case (Fig. 3). Equations 3.57, 3.58, 3.59 of the lecture notes have been used for the model geometry. The numerical results obtained are:

	Distances			
Diffracted ray	$d = 15,26m$	$s1 = 10,44m$	$s2 = 5,83m$	$\Delta r = 1,01m$

The Fresnel diffraction parameter, according to equation 3.57 of the lec-

ture notes, is:

$$\nu = 18,6833 \tag{4}$$

Thus the total P_{RX} (1) becomes:

$$P_{RX,NLOS} = \frac{1}{8R_a}\left(\frac{\lambda}{\pi}\right)^2 (60 \cdot EIRP)\left||F(\nu)|e^{j\cdot arg(F(\nu))}\frac{e^{-j\beta(s1+s2)}}{s1+s2}\right|^2 \tag{5}$$

where $F(\nu)$ is the Fresnel function and the other parameters are the same as the LOS case. Substituting the parameters computed before, the total power received in dBm is:

$$P_{RX,NLOS,dBm} = 10\log_{10}\left(\frac{P_{RX,NLOS}}{0.001}\right) \simeq -87,9895[dBm] \tag{6}$$

Again, the C++ code was filled with the arbitrary parameters chosen to show the results depicted in Fig. 3 below:

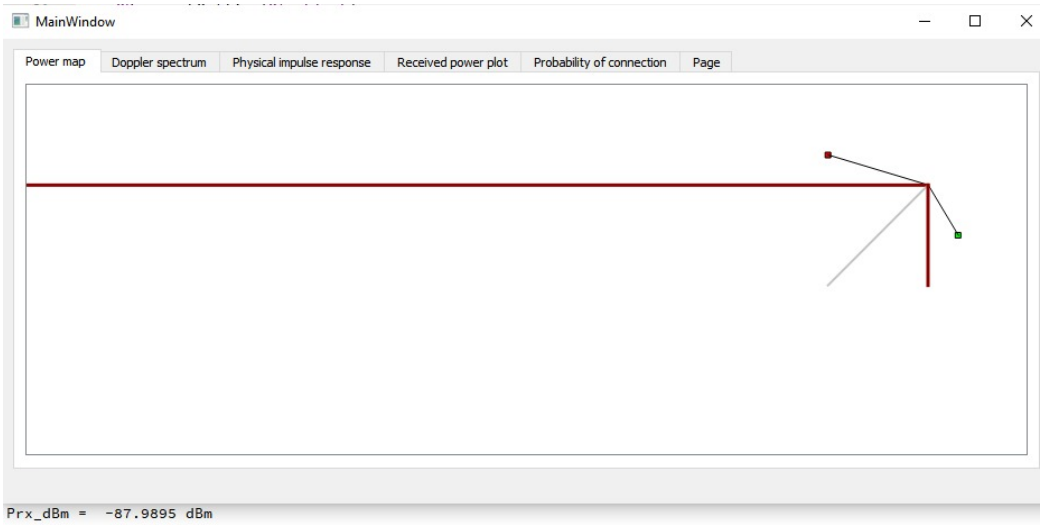

Figure 3: Diffraction results on Qt

The results perfectly match as expected.

4 Impulse responses

In a general point of view, the system is considered as a time-variant system with physical impulse response[4]:

$$h(\tau, t) = \sum_{n=1}^{N} \alpha_n(t)\delta(\tau - \tau_n) \tag{7}$$

Thanks to the quasi-static approximation, the physical channel is intended as time-invariant. This can be kept during all the transmissions considering that the time of a single transmission changes faster than the clock time. However, the Rx is limited due to its finite bandwidth that determines the resolution time $\Delta\tau$. Thus, the Tapped Delay Line model (TDL) of the impulse response[5] is used:

$$h_{TDL}(\tau, t) = \sum_{l=0}^{L} h_l(t)\delta(\tau - l\Delta\tau) \tag{8}$$

where L depends on the channel maximum propagation delay and h_l are the tap gains[6].

Assume the following example of a transmission with multi-path components where the Rx and Tx are 50m apart from each other, each on one side of the street:

[4]Eq. 1.12 of the lecture notes
[5]Eq. 1.20 of the lecture notes
[6]Eq. 1.22 of the lecture notes

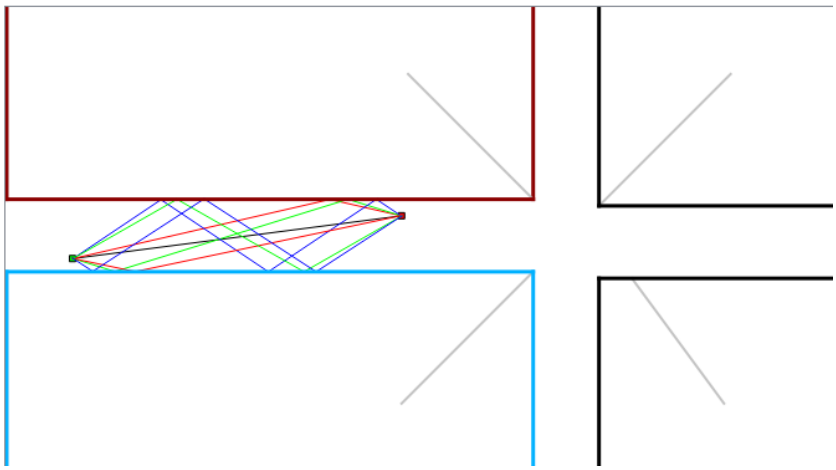

Figure 4: Simulation example

The TDL impulse response is plotted along with the physical impulse response at different bandwidth values to observe its effect:

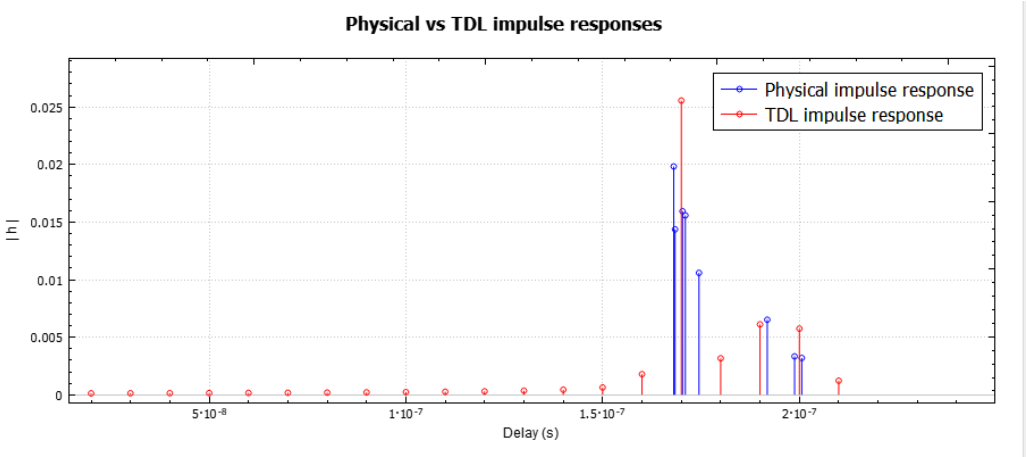

Figure 5: $B = 50MHz$, $\Delta\tau = 10ns$, delay spread $\sigma_\tau = 32.6ns$

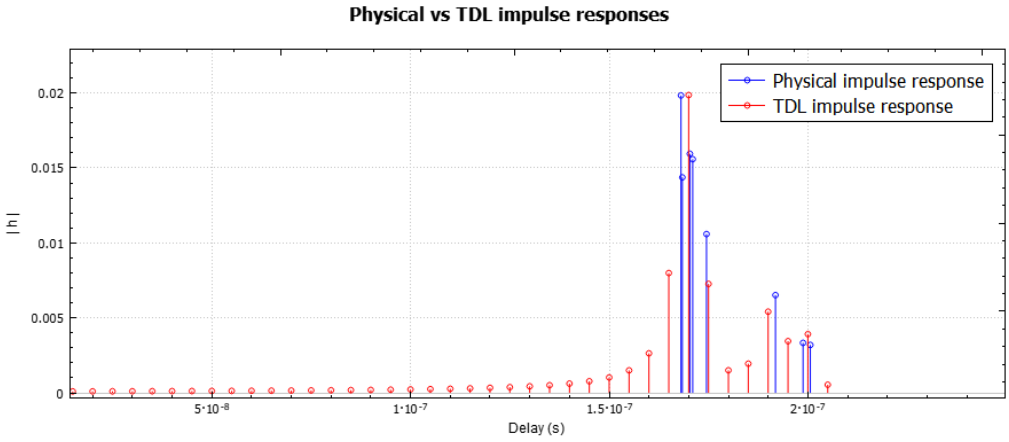

Figure 6: $B = 100MHz$, $\Delta\tau = 5ns$, delay spread $\sigma_\tau = 32.6ns$

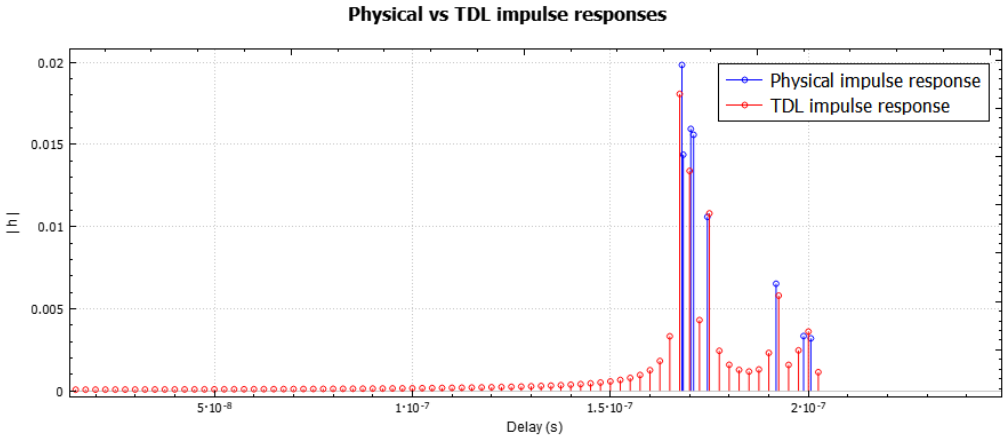

Figure 7: $B = 200MHz$, $\Delta\tau = 2.5ns$, delay spread $\sigma_\tau = 32.6ns$

As it is known from the theory, the delay spread[7] σ_τ is the time interval defined by the first signal component (the LOS one, if it exists) and the last arriving signal component (the longest of the multipaths) and it defines the length in which a single impulse applied at the input is spread over time at

[7]Eq. 1.25 of the lecture notes

the output. The channel coherence bandwidth[8] Δf_c is the inverse of the delay spread. It defines the range of frequencies where the channel can be assumed flat. Thus, if the signal bandwidth B is smaller than Δf_c, the signal can be received correctly because it will suffer only from flat fading. Otherwise, the fading will be selective and the signal will not be received because of the attenuation. From the Fig. 5, 6 and 7 can be clearly seen σ_τ that corresponds to the interval where the signal is present (received).

The assumption of *Uncorrelated Scattering* (US) is made by assuming that not all multi-path components contribute to each tap delay but fade sufficiently fast to consider they only contribute to the tap they are situated in[9]. The comparison with the physical impulse response is done again for different bandwidths:

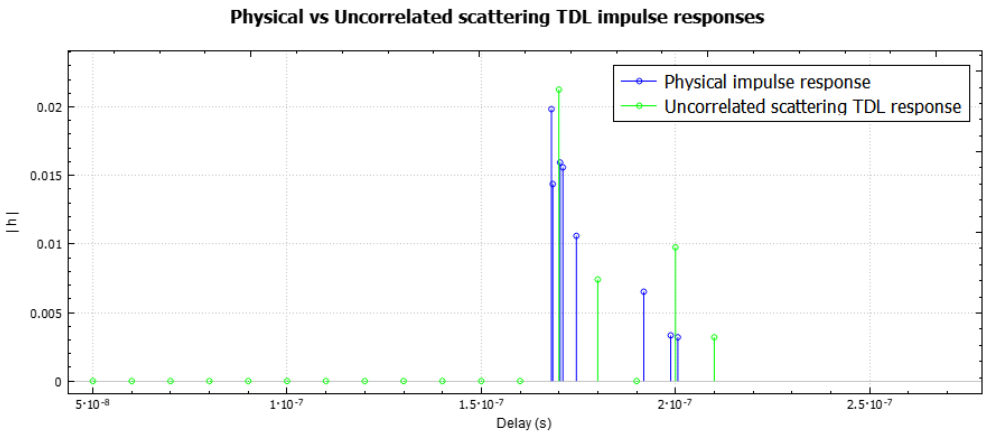

Figure 8: $B = 50MHz$, $\Delta\tau = 10ns$, delay spread $\sigma_\tau = 32.6ns$

[8]Eq. 1.25 of the lecture notes
[9]Eq. 1.23 of the lecture notes

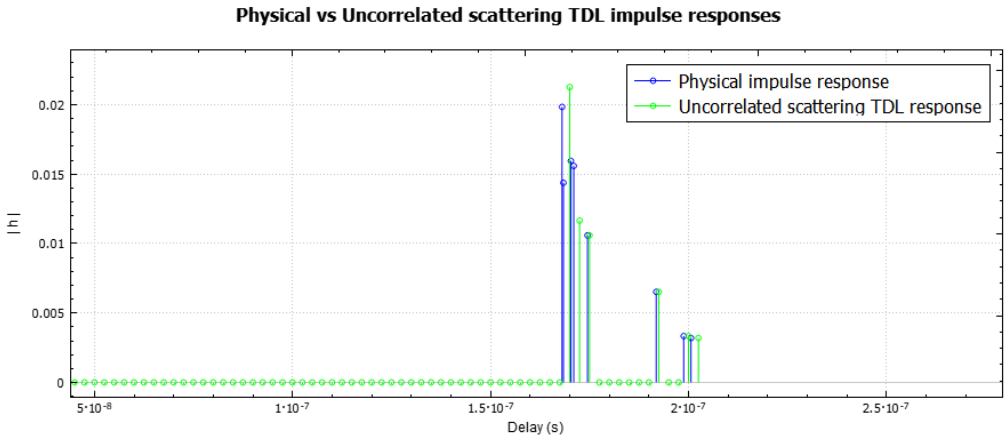

Figure 9: $B = 200MHz$, $\Delta\tau = 2.5ns$, delay spread $\sigma_\tau = 32.6ns$

5 Doppler spectrum

Let us consider the case of a mobile receiver moving at a speed v in some direction. This one will observe a Doppler effect for each component arriving at different angle from the speed direction. The global spectrum will contain therefore multiple replicas of the carrier frequency shifted by $\omega_D = \beta\ v\ cos(\theta)$. When the receiver moves, it experiences fading due to interference between the different components, and due to the fact that the channel response varies over time.

Let us take the example of Fig. 4 where the receiver on the left is moving in the positive x direction at a walking speed of $1m/s$, and in the y direction at a speed of $1.2m/s$ (crossing the street for example). The resulting spectrum is the following[10]:

[10]The plots show only the frequency shift value of the MPCs from the carrier frequency. This is due to a difficulty with the plot software to display values at the carrier level.

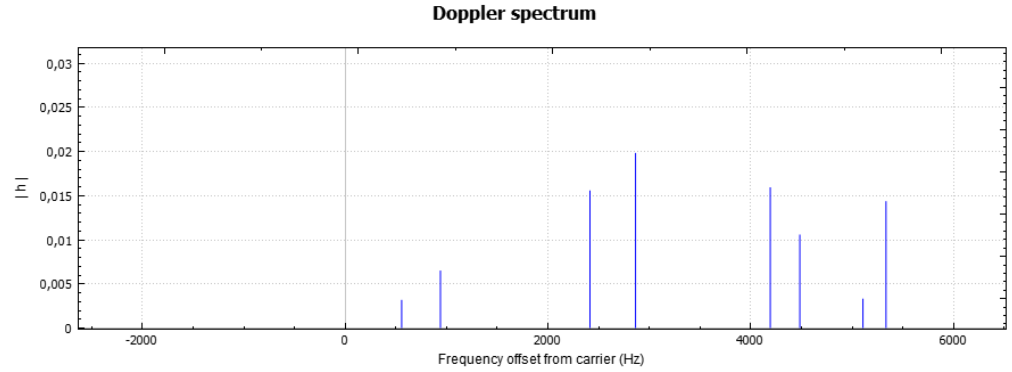

Figure 10: Max Doppler shift $= 5.344kHz$, coherence time $\Delta t_c = 3.69ms$

Another example below illustrates the spectrum if the mobile moves at a car speed ($\approx 50km/h$).

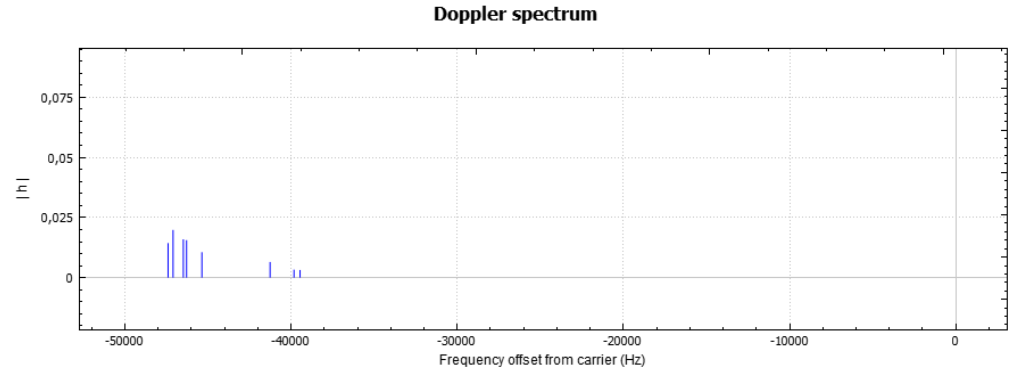

Figure 11: Max Doppler shift $= 4.749kHz$, coherence time $\Delta t_c = 0.41ms$

Fig. 10 and Fig. 12 give the maximum frequency shift obtainable (see captions) at those speeds, and the coherence times. Coherence time is a useful parameter since it corresponds to a time lapse during which the channel can be considered invariant. Therefore it is better to have a low coherence time for a better connection. As observed above, a high speed mobility makes connection more difficult.

6 Rice factor

The rice factor measures the power of the LOS component relatives to the others, $K = \frac{a_0}{\sum a_i}$. The bigger it is, the more tight the distribution of the impulse response $|h|$ is (PDF). The LOS components becomes more dominant and the receiver is subject to less fading.

For the example of Fig. 4 in which the transmitter and receiver are some $50m$ apart, the Rice factor is $K = 0.44$. In a configuration where they are closer, Rice factor is more important:

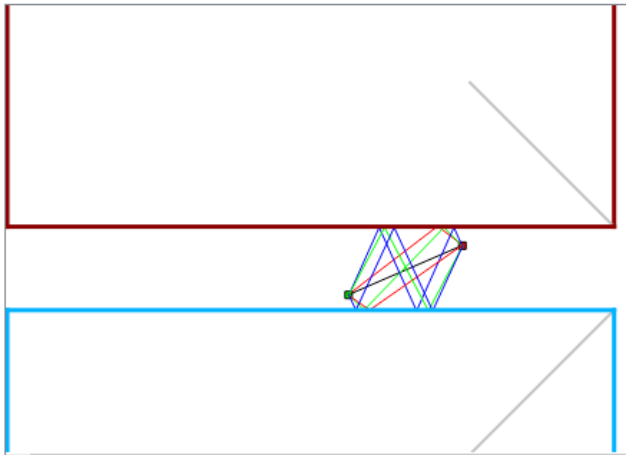

Figure 12: Rice factor $K = 1.55$

7 Path loss model

Note: this section, as well as sections 8, 9, 10 are illustrated with the simulation example of Fig. 13. The main street is $250m$ long, and each building block is $70m$ or $80m$ long. The crossing streets are close to $30m$ deep. The map has been designed with few desired inconsistencies to make an environment a bit diversified. Fig. 13 is a coloured map of the received power, with a colour gradient going from red ($\leq -25dBm$) to black ($\geq -100dBm$).

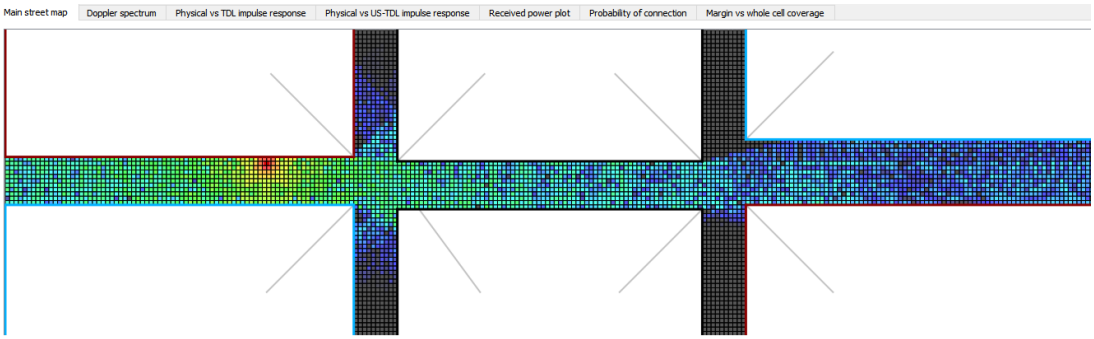

Figure 13: Simulation example

The path loss model is useful information whenever a cellular network is deployed to observe the coverage. It intends to observe the rate at which the received power decreases with the distance from the transmitting antenna. The model is given by the canonical expression:

$$P_{RX}(d)[dBm] = P_{RX}(d_0)[dBm] - 10\ n\ log(d/d_0) \tag{9}$$

This allows to characterise the environment studied and to compare it with a free space propagation, where the *path loss exponent* $n = 2$.

To describe the studied environment, a scattering plot of the received power in function of the distance has been made, and was then approached by a linear regression line (least square method) to obtained a linear form like equation (9), as shown in Fig. 14.

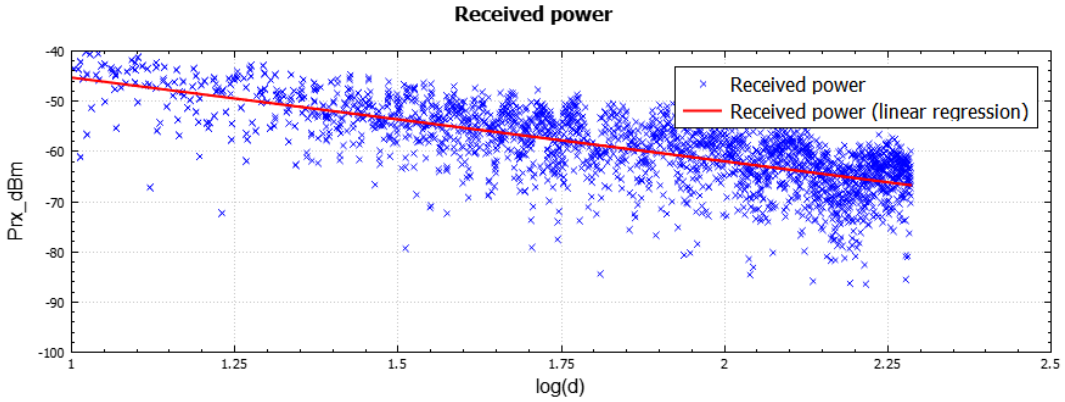

Figure 14: Scattering of the received power and linear approximation (red). Fading variability = 5.22 . Line equation: $y = -16.68x - 28.61$

The path loss exponent is found to be equal to $n \approx 1.67$. The fact that the path loss exponent is lower than in free space shows that the environment (ground included) is responsible for a "waveguide effect". Indeed the received power decreases less fast than in free space because the environment redirects waves to the receiver antenna.

8 Fading variability

With the results obtained at Fig. 14 we can have an expression for the average path loss:

$$< L(d)[dBm] > = P_{TX}[dBm] - < P_{RX}[dBm] > \tag{10}$$

Where $< P_{RX}[dBm] >$ is given by the linear approximation on Fig. 14. However, the model can be more accurate than by considering only the average path loss. Indeed, to mimic the real evolution of the path loss, models can take into account a statistical effect, *fading variability* L_{σ_L}, that is responsible for the deviations from the average curve.

$$L(d)[dBm] =< L(d)[dBm] > +L_{\sigma_L} \tag{11}$$

The variability is a log-normally distributed random variable and its standard deviation shown on Fig. 14 is $\sigma_L = 5.22$.

9 Cell coverage

It is in general desired to know what is the coverage of a cell around the base station.

9.1 Link Budget

The minimal allowed power for a connection can be determined by establishing a link budget in function of provided target parameters: target SNR ($SNR = 8dB$), receiver noise figure ($F_{dB} = 10dB$), thermal input noise power ($= 10\ log(kT_0B/1mW)$), and interference margin ($I_m = 6dB$)).

The Rx sensitivity RS is the minimal power required for a target data rate and is the sum (in dB) of the thermal noise power, the noise figure and SNR. The maximal allowed path loss is defined as $L_m = P_{TX} - (RS + I_m)$. Hereafter, $P_{RX,min} = (RS + I_m)$ is the minimum allowed received power, taking the interference margin into account.

9.2 Probability of connection

The connection probability can be defined as the probability that the maximum path loss is not exceeded $P[L(d) < L_m] = P[L_{\sigma_L} < L_m - \langle L(d)\rangle]$, which can be developed as:

$$1 - P[L_{\sigma_L} > L_m - \langle L(d)\rangle] = 1 - P[L_{\sigma_L} > \langle P_{RX}(d)\rangle - (RS - I_m)] \tag{12}$$

Since the fading variability is a random variable normally distributed, the last term of equation (12) can be computed by the error function giving $P[L_{\sigma_L} > \gamma]$ [11] using the variability σ_L found in the previous section results. The whole cell coverage can also be determined [12] and it is plotted along with the connection probability in Fig. 15.

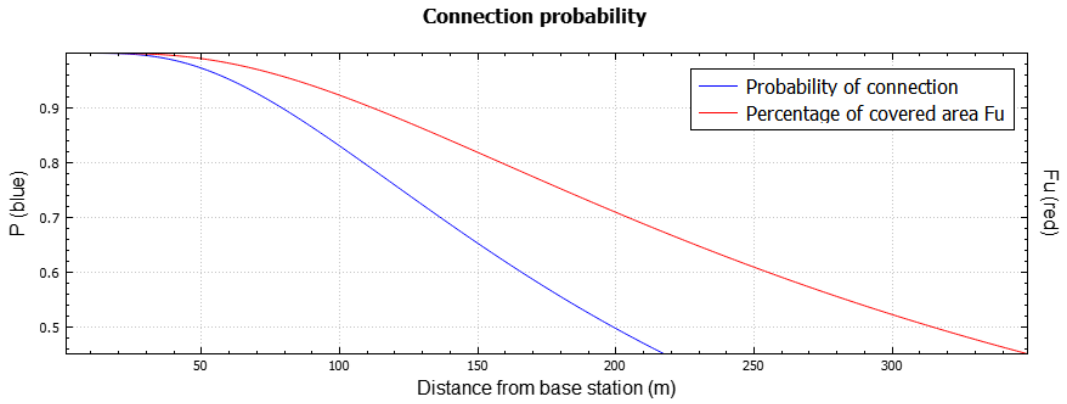

Figure 15: Connection probability

A plot of the whole cell coverage in function of the margin $L_m - L(d)$ is shown as well, in Fig. 16.

[11] See equation 3.69 of the lecture notes
[12] Equation 3.78 of the lecture notes

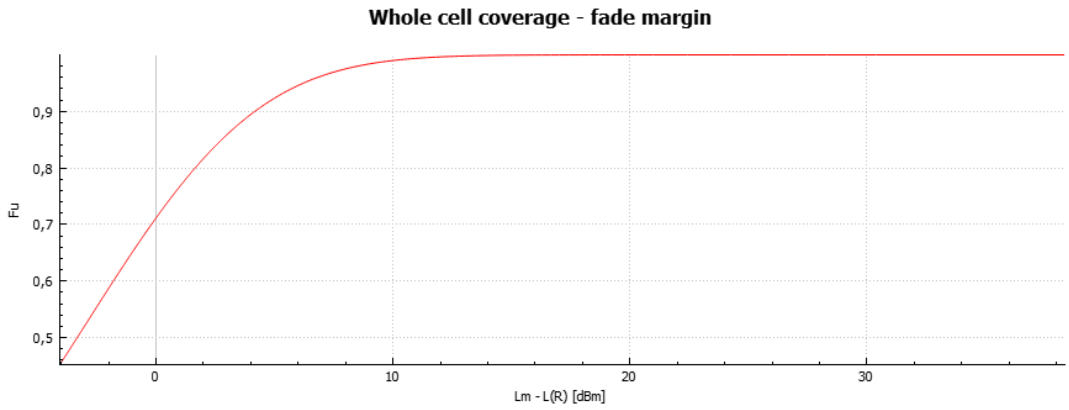

Figure 16: Percentage of the cell covered for a cell of radius R

The above result can be used to add a margin to the link budget for the maximal allowed path loss. One can observe in Fig.16 that if a typical 95% of the cell is desired to be covered, a margin of $7dB$ must be taken into account in the link budget. This margin is the *fade margin*.

10 Crossing streets coverage

For an arbitrarily placed base station as shown in the example in Fig. 13, the depth of coverage of a street can be evaluated. Note that the receiver is $30m$ away from the two first crossing streets.

The criteria applied here is the following: for each crossing street (four in total), the average power received over each horizontal section is computed. The depth of a street is defined by the maximum distance at which the averaged power still satisfies the link budget (as computed in section 9.1). Therefore the distance from the main street at which the average power falls below the minimal power allowed $P_{RX,min} = (RS - I_m)$ is considered as the depth of coverage[13]. For the example of Fig. 13, the program outputs the

[13] RS = receiver sensitivity, I_m = interference margin

following results on the console:

```
Street n°1 depth =  15 m
Street n°2 depth =  0 m
Street n°3 depth =  9 m
Street n°4 depth =  1 m
```

Figure 17: Depth of coverage output. Street 1 and 2 are respectively upper left and right crossing streets, and streets 3 and 4 are respectively lower left and right

11 Conclusion

In order to simulate and characterise a 5G small cells network, a C++ program of ray-tracing has been implemented. An old version of image method for ray-tracing purpose was re-used and improved to include diffraction.

The new features implemented were tested and checked by small scale examples. Once validated, they were used to simulate and model a larger example of typical city streets, crossing at right angles. The simulation allowed to establish different model of impulse responses, path loss and fading variability models, and to characterise the coverage of a 5G cell in such environment.

A number of interesting features could be added in the future, as a more user friendly and less time consuming GUI. Beam forming techniques could as well be implemented, especially since the future 5G networks are to be equipped with such technologies.

Appendices

Appendix 1 - More example of simulations